

## Preparing of $\text{CuCo}_2\text{O}_4$ compound by Sol-gel method and studying its structural properties

Areej Yousef\*  , Ibrahim Ismail  

Department of Chemistry, Faculty of Science, Al-Baath University, Homs, Syria.

\*Corresponding Author.

Received 07/06/2023, Revised 27/10/2023, Accepted 29/10/2023, Published Online First 20/02/2024,  
Published 01/09/2024



© 2022 The Author(s). Published by College of Science for Women, University of Baghdad.

This is an open-access article distributed under the terms of the [Creative Commons Attribution 4.0 International License](https://creativecommons.org/licenses/by/4.0/), which permits unrestricted use, distribution, and reproduction in any medium, provided the original work is properly cited.

### Abstract

The  $\text{CuCo}_2\text{O}_4$  compound has been prepared by the Sol-gel method starting with cobalt sulfate  $\text{CoSO}_4 \cdot 7\text{H}_2\text{O}$  and copper nitrate, using Pectin as a stabilizer. The samples have been annealed at different temperatures (400-1000°C) to produce  $\text{CuCo}_2\text{O}_4$ . Thermo-gravimetric analysis (TGA), Fourier transform infrared spectroscopy (FT-IR), Scanning Electron Microscope (SEM) and X-ray diffraction (XRD) techniques have been used to characterize the compositional properties of the prepared compound. The optimum temperature for synthesis is found at 600°C. According to X-ray diffraction patterns,  $\text{CuCo}_2\text{O}_4$  spinel has a face-centered cubic crystal (FCC) and belonged to the  $\text{Fd}3\text{m}$  space group. The lattice constants, unit cell volume, and number of formulas have been calculated. Their values are 8.044 Å, 520.49 Å<sup>3</sup>, and 8, respectively. It is found that the grain size of the compound is 17.4nm. The experimental results for d corresponded to the reference card values with an accuracy of 99.5% as a minimum. The theoretical and experimental density of the prepared compound have been calculated and the results are approximately identical. The differential thermal analysis curves showed five thermal effects, the most important of which are the exo-thermal peak at 390°C and end-thermal peak at 740°C, which indicate to start forming and decomposition of Cu respectively. The IR spectroscopy encouraged our results during the bonding vibrations of Co-O, Cu-O.

**Keywords:** Copper cobaltite, Mixed oxide, Pectin, Spinel, Sol-gel.

### Introduction

Spinel is an important family of mixed metal oxides, the standard chemical formula for spinel is  $\text{AB}_2\text{O}_4$ , where A and B are cations that occupy tetrahedral and octahedral sites, respectively. B is a trivalent atom whereas A is often a divalent atom. Only one-eighth of the tetrahedral sites and one-half of the octahedral sites are occupied by the cations<sup>1</sup>. Cobalt-based spinels  $\text{MCo}_2\text{O}_4$  (M = Ni, Cu, Zn, Mg, Mn, Cd, etc.) are an intriguing class of oxide ceramics with significant technological uses; they have been used extensively in fields like chemical sensors<sup>2-4</sup>, electrode material<sup>5,6</sup>, electrocatalysts<sup>7</sup>,

supercapacitor<sup>8</sup> and other related fields. Common methods for producing cobaltite include solid-state reactions<sup>9</sup>, coprecipitation<sup>10</sup>, hydrothermal<sup>11,12</sup>, combustion<sup>13,14</sup>, microwave<sup>15,16</sup> and sol-gel processes<sup>17-20</sup>. When the material is synthesized utilizing a solution-based technique, the drawbacks of solid-state methods, such as inhomogeneity, lack of stoichiometry control, high temperature, and poor surface area, are improved. Due to its benefit of creating pure and ultrafine powders at low temperatures, the sol-gel process is a practical and alluring method for manufacturing cobaltite spinels.

One of the most efficient and interesting transition metal oxides is copper cobaltite  $\text{CuCo}_2\text{O}_4$  which has a spinel structure. It has been extensively researched because of its applications in supercapacitors and gas sensors properties<sup>21-23</sup>. In the present investigation,  $\text{CuCo}_2\text{O}_4$  nanocrystals are made using the sol-gel method. Thermogravimetric analysis (TGA), X-ray diffraction (XRD), and Fourier transform infrared (FTIR) spectroscopy have all been used in characterization studies. The novelty in the research lies in utilization an organic compound (Pectin) as a stabilizer in the process of copper cobaltite preparation from mineral salts. The crystal structure of the as-prepared  $\text{CuCo}_2\text{O}_4$  is shown in Fig. 1. It is obvious to see that cobalt and copper atoms are distributed over the centers of the stacked octahedra and tetrahedra, while the oxygen atoms are

distributed over the corners of the octahedra and tetrahedra.

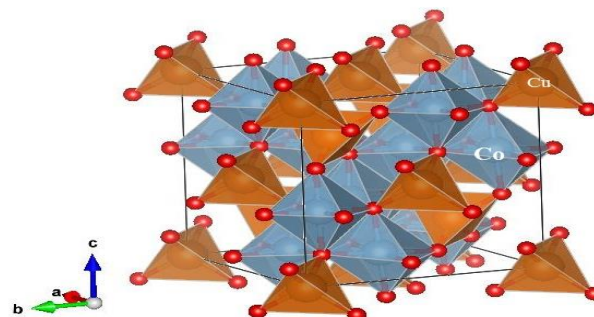
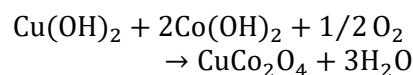
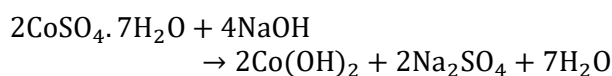
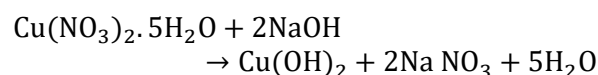


**Figure 1.** The unit cell of spinel structure of  $\text{CuCo}_2\text{O}_4$ .<sup>24</sup>

## Materials and Methods

Cobalt sulfate  $\text{CoSO}_4 \cdot 7\text{H}_2\text{O}$  (97% purity), copper nitrate  $\text{Cu}(\text{NO}_3)_2 \cdot 5\text{H}_2\text{O}$  (99% purity), Sodium hydroxide, Pectin, and distilled water. All chemicals used during the process of synthesis were purchased from Sigma-Aldrich, they were of analytical grade, and were used as received without any further purification. The  $\text{CuCo}_2\text{O}_4$  compound was synthesized by Sol-gel method, and appropriate amounts of starting materials (5.7959g)  $\text{CoSO}_4 \cdot 7\text{H}_2\text{O}$  and 2.4404g  $\text{Cu}(\text{NO}_3)_2 \cdot 5\text{H}_2\text{O}$  were separately dissolved in 100ml distilled water. Then, they were mixed for 30 min. Next, (2.4g) NaOH was dissolved in (100ml) distilled water and added to the mixed solution. (0.05g) of Pectin was added to the solution at room temperature under constant magnetic stirring for another 30 min. The resulting mixture solution was constantly stirred at 80°C for 1h until the gel was formed. After that, the gel was heated at 110°C until the formation of a powder. Subsequently, the as-prepared precursor was calcined at range of temperature (400-1000) °C for 6 h to obtain the  $\text{CuCo}_2\text{O}_4$  oxide. The weights of the starting materials used to form the  $\text{CuCo}_2\text{O}_4$  system were calculated by the following reactions:



Using a Differential Scanning Calorimeter (Shimadzu TG/DTA) with a ramp from 0 to 900°C at a heating rate of 30°C per min while nitrogen gas flowed, thermogravimetry differential thermal analysis (TG/DTA) was investigated. X-ray powder diffraction (XRD, Philips-PW-1840) with a Co-K radiation source  $\lambda=1.7889\text{\AA}$  and a scanning rate of  $0.02^\circ \text{ s}^{-1}$  in a  $2\theta$  range from 20 to 85° was used to carry out the structural characterization. ICDD standards were used in the analysis of the data. Using KBr pellet-based samples, an FTIR investigation was carried out using (Jascoo -FTIR) in the range of 4000 to  $400 \text{ cm}^{-1}$ , and the morphology of the obtained spinel oxides was explored using a Quanta 200 scanning electron microscope (SEM).

## Results and Discussion

### Thermal analysis

Fig. 2 depicts the  $\text{CuCo}_2\text{O}_4$  TG-DTA curve. The weight loss has been gradual and nearly totaled 90% of the overall precursor mass. The first loss of weight

starts around 95°C when lattice and adsorbed water begin to evaporate. The decomposition of the organic molecule may be responsible for the weight loss at temperatures between 250 and 390 °C, which marks the second stage of weight loss. A stable oxide may

have formed at 390°C because no further weight loss is noticed. Four endothermic peaks can be seen on the DTA curve. The loss of lattice water and adsorption water is responsible for the two peaks positioned below 250°C, while the organic compounds decomposition is responsible for the third peak at 280°C, and the last at 470°C indicates the dissociation of the compound. The level of DTA is exothermic above 390°C and almost completely lacks a counterpart on TG, which indicates the presence of solid-state processes that produce CuCo<sub>2</sub>O<sub>4</sub>

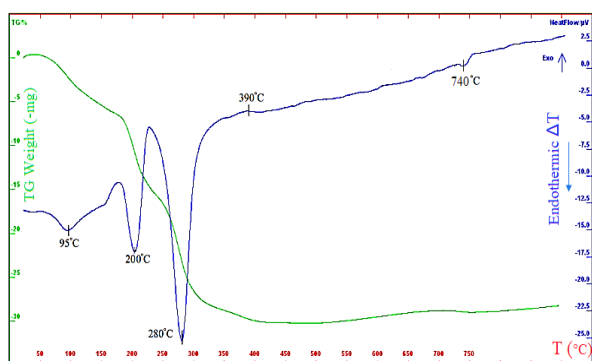


**Figure 2.** TG–DTA curve of CuCo<sub>2</sub>O<sub>4</sub> precursor material.

### X-ray diffraction (XRD) analysis

The XRD technique is a very useful tool to determine the phase, crystallinity and, purity of the samples prepared under various conditions<sup>25</sup>. Fig. 3 illustrates the XRD patterns of CuCo<sub>2</sub>O<sub>4</sub> which have been synthesized by the sol-gel method and annealed at different temperatures for 6 hours.

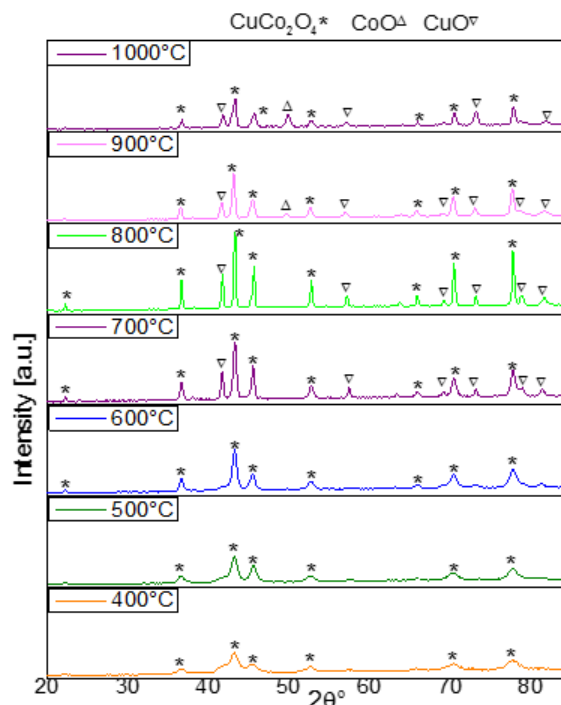


**Figure 3.** XRD patterns of the CuCo<sub>2</sub>O<sub>4</sub> following calcination at various temperatures.

It has been found that the compound started formation at 400°C, and by increasing the temperature from 400 to 600°C, the XRD peak intensity of CuCo<sub>2</sub>O<sub>4</sub> spinel increases stepwise. Meanwhile, the particle size of CuCo<sub>2</sub>O<sub>4</sub> increases with the sintering temperature and an obvious grain growth occurs mainly at 600°C. All diffraction peaks at 600°C are attributed to the CuCo<sub>2</sub>O<sub>4</sub> compound, and no peaks are related to copper oxide or cobalt oxide. The observed peaks at 2θ = (41.7, 57.5, 69.1, 73.1 and 78.9) above 600°C correspond with a second phase CuO (JCPDS No: 05-0661) this indicates that spinel started dissociation above this temperature. The previous discussion suggests that 600°C is the ideal temperature for the synthesis CuCo<sub>2</sub>O<sub>4</sub> compound where the peaks intensities are higher than those observed when calcining at 400°C and 500°C. All diffraction peaks observed at 600°C indicate the characteristic peak of the cubic CuCo<sub>2</sub>O<sub>4</sub>, with the spinel structure (ICCD No: 00-001-1155) and space group Fd3m. The face-centered cubic spinel structure can be precisely indexed to the diffraction peaks. Fig. 4 shows the XRD pattern of CuCo<sub>2</sub>O<sub>4</sub> compound that calcined at 600°C with (hkl) index. Eq. 1 gives the relation between lattice parameters and the d-spacing for the cubic system<sup>26</sup>:

$$\frac{1}{d^2} = \frac{h^2 + k^2 + l^2}{a^2} \dots\dots\dots 1$$

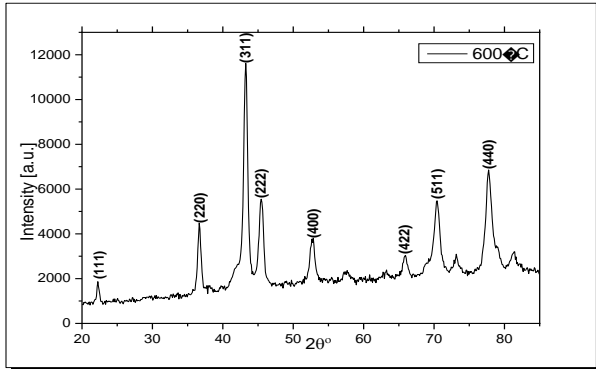


**Figure 4. XRD patterns of the CuCo<sub>2</sub>O<sub>4</sub> at 600°C**

Table 1 shows the diffraction angles, inter-planar distances, and Muller indexes that are calculated from the XRD pattern. The basic unit cell volume has been calculated using the relation:  $V = a^3$ . The flask density method (picknometer) has been used to measure the experimental density  $\rho_t$  of the prepared material<sup>27</sup>. Depending on the material's density, the number of formulas in a single crystalline cell  $Z$  is calculated by Eq. 2<sup>28</sup>:

$$\rho = \frac{MZ}{N_a V} \dots\dots\dots 2$$

Where  $M$  molecular weight of the material,  $N_a$  Avogadro number, and  $V$  basic unit cell volume (cm)<sup>3</sup>, it is found that:

$$Z = \frac{\rho \cdot N_a \cdot V}{M} = 8.00338 \approx 8$$

Using the rounding method, it is found that  $Z = 8$ , and therefore the general formula for the content of the basic unit cell can be written as follows: Cu<sub>8</sub>Co<sub>16</sub>O<sub>32</sub>. The broadening of diffraction lines may signify the nanoscale character of the component crystallites; Eq. 3 refers to Scherrer equation<sup>29-31</sup>:

$$D = \frac{K \lambda}{\beta \cos \theta} \dots\dots\dots 3$$

$D$  is the grain size,  $K$  is a constant equal to 0.9  $\lambda$  is the wavelength of the X-ray,  $\theta$  is the Bragg's diffraction angle (43.25, 45.48, 52.81, 65.9, 70.43, 77.70) and  $\beta$  is the full width at half maximum of the peak in radians.

Confirmed that the average crystal grain size is 17.4 nm, the obtained results are presented in Table 2.

**Table 1. Diffraction angle, inter planar, distance, R% and Muller indexes of CuCo<sub>2</sub>O<sub>4</sub> calcined at 600°C .**

2 $\theta$	I%	d <sub>exp</sub> A°	d <sub>card</sub> A°	R%	hkl
22.29	9	4.626	4.650	100	111
36.66	30	2.844	2.850	100	220
43.25	100	2.427	2.430	100	311
45.48	38	2.314	3.310	99.8	222
52.81	19	2.011	2.010	99.9	400
65.90	9	1.645	1.640	99.6	422
70.43	30	1.551	1.550	99.9	511
77.70	39	1.426	1.420	99.5	440

**Table 2. Lattice constants, unit cell volume, density, Z and crystallite size of CuCo<sub>2</sub>O<sub>4</sub> calcined at 600°C .**

a Å	V (Å) <sup>3</sup>	$\rho^E$ g.cm <sup>-3</sup>	$\rho_t$ g.cm <sup>-3</sup>	Z	D nm
8.044	520.49	6.272	6.263	8	17.4

**Scanning Electron Microscope SEM**

Fig. 5 shows SEM image of the CuCo<sub>2</sub>O<sub>4</sub> synthesized by sol-gel and calcined at 600°C. The images exhibit some heterogeneity in the distribution of the particles on surface. The shape of the microparticles is spherical.

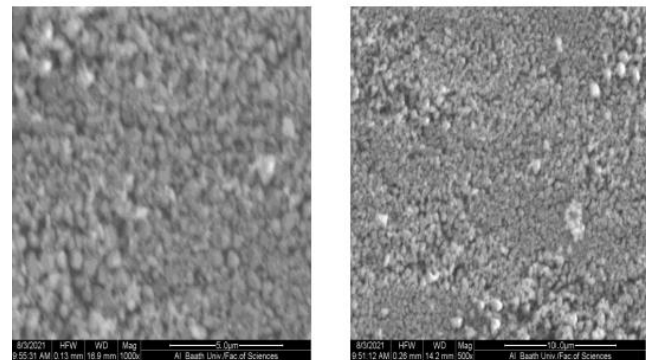


**Figure 5. SEM image of CuCo<sub>2</sub>O<sub>4</sub> calcined at 600°C .**

**Fourier Transform Infrared Spectroscopy**

CuCo<sub>2</sub>O<sub>4</sub> FT-IR spectrum is depicted in Fig. 6. The metal-oxygen stretching frequencies are ascribed to FT-IR spectra in the 400-1000 cm<sup>-1</sup> range<sup>32</sup>. Cu-O and Co-O such metal-oxygen stretching and bending vibrations can be attributed to two strong peaks with respective centers at 665.32 and 577.58 cm<sup>-1</sup><sup>33</sup>. The OH stretching and bending modes of adsorbed water molecules are shown by the bands at 3436.6 and 1626.66 cm<sup>-1</sup>, respectively<sup>34</sup>.

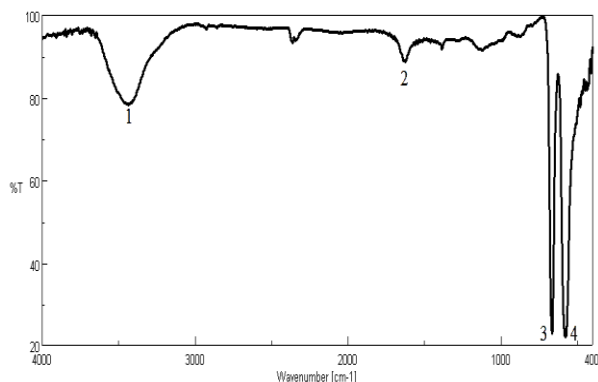


**Figure 6.** FTIR spectra of  $\text{CuCo}_2\text{O}_4$  calcined at  $600^\circ\text{C}$ .

## Conclusion

Spinel nanopowders can be produced using the sol-gel technique. It is incredibly easy, cheap, and produces materials with good characteristics at the nanoscale. Sol-gel technique has been used to successfully create the pure  $\text{CuCo}_2\text{O}_4$  nanopowders using Pectine as a stabilizer, which shows a spinel phase structure.  $\text{CuCo}_2\text{O}_4$  spinel's XRD peak

intensity rises stepwise as the sintering temperature rises from  $400$  to  $600^\circ\text{C}$ . Meanwhile,  $\text{CuCo}_2\text{O}_4$  particle size grows as the sintering temperature rises, with a clear grain growth occurring mostly at  $600^\circ\text{C}$ . It is built in a cubic shape.  $\text{CuCo}_2\text{O}_4$  crystals calcined at  $600^\circ\text{C}$  had a size of around  $17.4\text{nm}$ .

## Acknowledgment

The authors are grateful to Dr. Abba Alzoubi and Dr. Rasha Yousef the technical team in XRD Lab at Al-Baath University, Homs, Syria for XRD

experiments. The authors also acknowledge the Writefull Revise website in Hindawi for reviewing and revising my manuscript

## Authors' Declaration

- Conflicts of Interest: None.
- We hereby confirm that all the Figures and Tables in the manuscript are ours. Furthermore, any Figures and images, that are not ours, have been

included with the necessary permission for republication, which is attached to the manuscript.

- Ethical Clearance: The project was approved by the local ethical committee at University of Al-Baath University.

## Authors' Contribution Statement

A.Y. worked at conceptualization, methodology, acquisition of data, interpretation, drafting the MS, and designing original draft preparation. I.I. worked

at visualization, investigation, editing, analysis, revision, and proofreading.

## References

1. Poongodi R, Senguttuvan S, Sagayaraj R. AJ Csian urnal of hemistry AJ Csian urnalof hemistry. Asian J Chem. 2023; 35(6): 1525-32. <https://doi.org/10.14233/ajchem.2023.27625>
2. Zhou T, Cao S, Zhang R, Tu J, Fei T, Zhang T. Effect of cation substitution on the gas-sensing performances of ternary spinel  $\text{MCo}_2\text{O}_4$  ( $\text{M} = \text{Mn}, \text{Ni}$ , and  $\text{Zn}$ ) multishelled hollow twin spheres. ACS Appl Mater. Interfaces 2019 Jul 10; 11(31): 28023-32. <https://doi.org/10.1021/acsami.9b07546>
3. Gonçalves JM, Rocha DP, Silva MN, Martins PR, Nossol E, Angnes L, et al. Feasible strategies to promote the sensing performances of spinel  $\text{MCo}_2\text{O}_4$  ( $\text{M} = \text{Ni}, \text{Fe}, \text{Mn}, \text{Cu}$  and  $\text{Zn}$ ) based electrochemical



- sensors: a review. *J Mater Chem C Mater*. 2021; 9(25): 7852-87. <https://doi.org/10.1039/d1tc01550h>
- Alali KT, Liu J, Liu Q, Li R, Zhang H, Aljebawi K, et al. Enhanced acetone gas sensing response of ZnO/ZnCo<sub>2</sub>O<sub>4</sub> nanotubes synthesized by single capillary electrospinning technology. *Sens Actuators B Chem*. 2017 Nov 1; 252: 511-22. <https://doi.org/10.1016/j.snb.2017.06.034>
  - Patel AR, Sereda G, Banerjee S. Synthesis, characterization and applications of spinel cobaltite nanomaterials. *Curr Pharm Biotechnol*. 2021 May 1; 22(6): 773-92. <https://doi.org/10.2174/1389201021666201117122002>
  - Kavinkumar T, Vinodgopal K, Neppolian B. Development of nanohybrids based on porous spinel MCo<sub>2</sub>O<sub>4</sub> (M= Zn, Cu, Ni and Mn)/reduced graphene oxide/carbon nanotube as promising electrodes for high performance energy storage devices. *Appl Surf Sci*. 2020 May 30; 513: 145781. <https://doi.org/10.1016/j.apsusc.2020.145781>
  - Tan P, Wu Z, Chen B, Xu H, Cai W, Jin S, et al. Cation-substitution-tuned oxygen electrocatalyst of spinel cobaltite MCo<sub>2</sub>O<sub>4</sub> (M= Fe, Co, and Ni) hexagonal nanoplates for rechargeable Zn-air batteries. *J Electrochem Soc*. 2019 Oct 11; 166(14): A3448. <https://doi.org/10.1149/2.1311914jes>
  - Puratchi Mani M, Ponnarasi K, Rajendran A, Venkatachalam V, Thamizharasan K, Jothibas M. Electrochemical behavior of an advanced FeCo<sub>2</sub>O<sub>4</sub> electrode for supercapacitor applications. *J Electron Mater*. 2020 Oct; 49: 5964-9. <https://doi.org/10.1007/s11664-020-08296-3>
  - Martín-González MS, Fernández JF, Rubio-Marcos F, Lorite I, Costa-Krämer JL, Quesada A, et al. Insights into the room temperature magnetism of ZnO/Co<sub>3</sub>O<sub>4</sub> mixtures. *J Appl Phys*. 2008 Apr 15; 103(8): 083905. <https://doi.org/10.1063/1.2904862>
  - Li K, Li T, Dai Y, Quan Y, Zhao J, Ren J. Highly active urchin-like MCo<sub>2</sub>O<sub>4</sub> (M= Co, Cu, Ni or Zn) spinel for toluene catalytic combustion. *Fuel (Lond)*. 2022 Jun 15; 318: 123648. <https://doi.org/10.1016/j.fuel.2022.123648>
  - Pore OC, Fulari AV, Shejwal RV, Fulari VJ, Lohar GM. Review on recent progress in hydrothermally synthesized MCo<sub>2</sub>O<sub>4</sub>/rGO composite for energy storage devices. *Chem Eng J*. 2021 Dec 15; 426: 131544. <https://doi.org/10.1016/j.cej.2021.131544>
  - Cheng X, Zhou X, Liu Z, Zhang Y, Liu Q, Li B, et al. Hydrothermal solvothermal synthesis and microwave absorbing study of MCo<sub>2</sub>O<sub>4</sub> (M= Mn, Ni) microparticles. *Npj Mater Degrad*. 2019 Nov 17; 118(8): 466-72. <https://doi.org/10.1080/17436753.2019.1667174>
  - Yang Y, Gong J, Cai D, Li Y, Sun Y, Wang W, et al. Flexible synthesis of CuCo<sub>2</sub>O<sub>4</sub> hexagonal nanocrystal by melting salt modified combustion method as high-performance anode materials for lithium-ion batteries. *J Electroceram*. 2023 May; 50(3): 57-66. <https://doi.org/10.1007/s10832-023-00305-1>
  - Deraz NM, Fouda MM. Fabrication and magnetic properties of cobalt-copper nano composite. *Int J Electrochem. Sci*. 2013 Feb 1; 8(2): 2682-90. [https://doi.org/10.1016/S1452-3981\(23\)14340-9](https://doi.org/10.1016/S1452-3981(23)14340-9)
  - Harada M, Kotegawa F, Kuwa M. Structural changes of spinel MCo<sub>2</sub>O<sub>4</sub> (M= Mn, Fe, Co, Ni, and Zn) electrocatalysts during the oxygen evolution reaction investigated by in situ X-ray absorption spectroscopy. *ACS Appl Energy Mater*. 2022; 5(1): 278-94. <https://doi.org/10.1021/acsaem.1c02824>
  - Siveswari A, Gowthami V. Enhanced electrochemical performance of rod-like NiO and porous SnO<sub>2</sub> embedded NiCo<sub>2</sub>O<sub>4</sub> heterostructures as super capacitor electrode. *Neuroquantology*. 2022; 20(16): 4434. <https://doi.org/10.48047/NQ.2022.20.16.NO880449>
  - Rekhila G, Saidani A, Hocine F, Hariz SH, Trari M. Characterization of the hetero-system ZnCo<sub>2</sub>O<sub>4</sub>/ZnO prepared by sol gel: Application to the degradation of Ponceau 4R under solar light. *Appl Phys A Mater Sci Process*. 2020; 126: 1-8. <https://doi.org/10.1007/s00339-020-03766-1>
  - Guragain D, Zequine C, Gupta RK, Mishra SR. Facile synthesis of bio-template tubular MCo<sub>2</sub>O<sub>4</sub> (M= Cr, Mn, Ni) microstructure and its electrochemical performance in aqueous electrolyte. *Processes (Basel)*. 2020; 8(3): 343. <https://doi.org/10.3390/pr8030343>
  - Lobo LS, Kumar AR. Structural and electrical properties of ZnCo<sub>2</sub>O<sub>4</sub> spinel synthesized by sol-gel combustion method. *J Non Cryst Solids*. 2019; 505: 301-9. <https://doi.org/10.1016/j.jnoncrysol.2018.11.004>
  - Liu L, Li Y, Pang Y, Lan Y, Zhou L. Activation of peroxy monosulfate with CuCo<sub>2</sub>O<sub>4</sub>@ kaolin for the efficient degradation of phenacetin. *Chem Eng J*. 2020; 401: 126014. <https://doi.org/10.1016/j.cej.2020.126014>
  - George A, Kundu M. Construction of self-supported hierarchical CuCo<sub>2</sub>O<sub>4</sub> dendrites as faradaic electrode material for redox-based supercapacitor applications. *Electrochim Acta*. 2022; 433: 141204. <https://doi.org/10.1016/j.electacta.2022.141204>
  - Sun J, Xu C, Chen H. A review on the synthesis of CuCo<sub>2</sub>O<sub>4</sub>-based electrode materials and their applications in supercapacitors. *J Mater*. 2021; 7(1): 98-126. <https://doi.org/10.1016/j.jmat.2020.07.013>
  - Zhao Z, Deng Z, Zhang R, Klamchuen A, He Y, Horprathum M, et al. Sensitive and selective ozone sensor based on CuCo<sub>2</sub>O<sub>4</sub> synthesized by a facile solution combustion method. *Sens Actuators B Chem*. 2023; 375: 132912. <https://doi.org/10.1016/j.snb.2022.132912>
  - Wyckoff RWG, Zussman JR. *Crystal Structures. Miscellaneous Inorganic Compounds, Silicates, and*

- Basic Structural Information. Chichester and New York (Wiley: Interscience), 1968; 2nd Ed, vol 4: 566 pp.  
<https://doi.org/10.1180/minmag.1969.037.288.28>
25. Merabet L, Rida K, Boukmouche N. Sol-gel synthesis, characterization, and supercapacitor applications of MCo<sub>2</sub>O<sub>4</sub> (M= Ni, Mn, Cu, Zn) cobaltite spinels. *Ceram Int.* 2018; 44(10): 11265-73.  
<https://doi.org/10.1016/j.ceramint.2018.03.171>
26. Smart LE, Moore EA. *Solid State Chemistry*. 3rd ed. Boca Raton London New York Singapore: Taylor & Francis Group, LLC; 2005.  
<https://www.pdfdrive.com/solid-state-chemistry-e13884425html>
27. Agnew JM, Leonard JJ, Feddes J, Feng Y. A modified air pycnometer for compost air volume and density determination. *Can Biosyst Eng.* 2003; 45: 6-27.
28. WEST AR. *Solid State Chemistry and its Applications*. 2nd ed. University of Sheffield, UK: John Wiley & Sons, Lt; 2014.
29. Abaide ER, Anchieta CG, Foletto VS, Reinehr B, Nunes LF, Kuhn RC, et al. Production of copper and cobalt aluminate spinels and their application as supports for inulinase immobilization. *Mater Res.* 2015; 1062-9. <https://doi.org/10.1590/1516-1439.031415>
30. Ali M, Abbas A, Drea A. Green synthesis of nano binary oxide SiO<sub>2</sub>/V<sub>2</sub>O<sub>5</sub> NPs integrated ointment cream application on wound dressings and skin cancer cells. *Baghdad Sci J.* 2023; 20(3): 734-745.  
<https://doi.org/10.21123/bsj.2022.7318>
31. Shaker DS, Abass NK, Ulwall RA. Preparation and study of the Structural, Morphological and Optical properties of pure Tin Oxide Nanoparticle doped with Cu. *Baghdad Sci J.* 2022; 19(3): 0660-.  
<https://dx.doi.org/10.21123/bsj.2022.19.3.0660>
32. Yuvasravana R, George PP, Devanna N. A Green-Chemical Approach for the Synthesis of Cobaltate Spinel Mco<sub>2</sub>o<sub>4</sub> [M= Mg and Ni] under Microwave Assistance. *Int J Innov Res Technol Sci. Eng. Tech.* 2017; 6: 11256.  
<https://doi.org/10.15680/IJRSET.2017.0606208>
33. Heiba ZK, Farag NM, El-Naggar AM, Abdellatif M, Aldhafiri AM, Mohamed MB, et al. Effect of Mo-doping on the structure, magnetic and optical characteristics of nano CuCo<sub>2</sub>O<sub>4</sub>. *J Mater Res Technol.* 2021; 10: 832-9.  
<https://doi.org/10.1016/j.jmrt.2020.12.056>
34. Thendral KT, Amutha M, Ragunathan R. Design and development of copper cobaltite (CuCo<sub>2</sub>O<sub>4</sub>) nanoparticle for antibacterial anticancer and photocatalytic activity. *Mater Lett.* 2023; 134720.  
<https://doi.org/10.1016/j.matlet.2023.134720>

## اصطناع المركب CuCo<sub>2</sub>O<sub>4</sub> بطريقة الـ Sol-gel ودراسة خواصه التركيبية

أريج يوسف، إبراهيم اسماعيل

قسم الكيمياء، كلية العلوم، جامعة البعث، حمص، سوريا.

### الخلاصة

تم في هذا البحث تحضير مركب كوبالتيت النحاس CuCo<sub>2</sub>O<sub>4</sub> بطريقة الـ Sol-Gel انطلاقاً من ملح كبريتات الكوبالت و نترات النحاس. تم استخدام مركب عضوي هو اليكتين كعامل تثبيت أعطى استقراراً عالي لجملة الهيدروكسيدات أثناء التحضير. تم حرق العينة المحضرة عند درجات حرارة مختلفة ضمن المجال (400-1000°C) لتحديد درجة الحرارة الأفضل للحصول على البلورات المطلوبة من المركب CuCo<sub>2</sub>O<sub>4</sub>. درست الخواص التركيبية للأكسيد المحضّر باستخدام تقنية انعراج الأشعة السينية (XRD) وجهاز التحليل الحراري التفاضلي (DTA)، ومطيافية تحت الأحمر (IR)، والمجهر الإلكتروني الماسح (SEM). تم تحديد درجة حرارة الاصطناع المثلى عند الدرجة 600°C. بينت دراسة مخططات انعراج الأشعة السينية أن المركب يتبلور وفق بنية بلورية مكعبية متمركزة الوجوه FCC من نمط السباينل ومجموعة تناظر فراغية S.G هي Fd3m. حُسبت ثوابت الشبكة وحجم التبلور وعدد الصيغ للمركب المحضّر وكانت 8.044 Å<sup>3</sup>، 520.49 Å<sup>3</sup>، 8 على الترتيب. تبين أن حجم الحبيبات للمركب هو 17.4nm. تطابقت الحسابات التجريبية لـ d مع قيم الطاقة المرجعية بنسبة تطابق 99.5% كحد أدنى. حسب الكثافة النظرية والتجريبية للمركب المحضّر وكانت النتائج متقاربة. أظهرت منحنيات التحليل الحراري التفاضلي إلى وجود خمس آثار حرارية أهمها الأثر الحراري الناشر عند الدرجة 390°C والأثر الحراري الماص عند الدرجة 740°C اللذان يشيران إلى بدء تشكل المركب وبدء تفككه على الترتيب. يؤكد مخطط الطيف تحت الأحمر (IR) الحصول على المركب المطلوب من خلال القمم العائدة لاهتزازات الروابط (Co-O) و (Cu-O).

الكلمات المفتاحية: كوباتات النحاس، أكاسيد مختلطة، اليكتين، Sol-gel، سباينل.